Organic/Inorganic Langmuir−Blodgett Films Based on Metal Phosphonates. 5. A Magnetic Manganese Phosphonate Film Including a Tetrathiafulvalene Amphiphile[1]

Melissa A. Petruska,[†] Brian C. Watson,[‡] Mark W. Meisel,[‡] and Daniel R. Talham*[,†]

Department of Chemistry, University of Florida, P. O. Box 117200, Gainesville, Florida 32611-7200, and Department of Physics and Center for Condensed Matter Sciences, University of Florida, P. O. Box 118440, Gainesville, Florida 32611-8440

Received July 3, 2001. Revised Manuscript Received February 20, 2002

Mixed organic/inorganic Langmuir−Blodgett (LB) films have been prepared in which the polar network is a manganese phosphonate continuous lattice and the organic network contains a substituted tetrathiafulvalene amphiphile. The bis(phosphonic acid) amphiphile, 2,3-bis[(4′-phosphonobutyl)thio]-6,7-bis(tetradecylthio)tetrathiafulvalene, **1**, has been synthesized and deposited from an aqueous Mn^{2+} subphase to form Y-type LB films with stoichiometry $Mn_2(\mathbf{1})(H_2O)_2$. Since the amphiphile is a bis(phosphonate), the inorganic network forms the $Mn(O_3PR)H_2O$ structure known in other manganese phosphonate LB films and layered solids. The film becomes magnetic near 11.5 K when the manganese phosphonate network orders as a canted antiferromagnet. Attempts to subsequently oxidize the tetrathiafulvalene (TTF) network did not result in stable phases. Structural characterization was aided by the synthesis of a solid-state manganese bis(phosphonate) model compound, $Mn_2(\mathbf{2})(H_2O)_2$, where **2** is the ligand 2,3-bis[(2′-phosphonoethyl)thio]-6,7-bis(methylthio)-tetrathiafulvalene.

Introduction

Langmuir−Blodgett (LB) films are traditionally layered organic assemblies that are first formed at the air−water interface and then transferred to a solid support.[2−4] This process normally results in a two-dimensional crystalline or liquid crystalline array of organic amphiphiles. We have recently developed methods to incorporate inorganic networks into LB films to produce mixed organic/inorganic monolayers and multilayers.[5−15] The LB films incorporate two-dimensional metal phosphonate lattices and are modeled after known layered solid-state phases. An advantage of the mixed organic/inorganic LB films is that properties typical of the inorganic solid state can now be included while the elegance of LB deposition is retained. For example, we have recently demonstrated that metal phosphonate LB films are significantly more stable than traditional LB films because of the inorganic lattice.[1] We have also demonstrated magnetic order in manganese phosphonate LB films.[9,12,16]

Manganese(2+), as well as several other divalent metal ions, form layered structures of general formula $M(O_3PR)H_2O$ with organophosphonates (Figure 1).[17−19] In the inorganic layer, manganese ions are bridged by phosphonate oxygens to form a nearly square grid lattice.[18] Each metal ion is coordinated by five phosphonate oxygens and a water of hydration, resulting in a distorted octahedral coordination environment. At low

* To whom correspondence should be addressed.
[†] Department of Chemistry.
[‡] Department of Physics and the Center for Condensed Matter Sciences.

(1) Petruska, M. A.; Talham, D. R. *Langmuir* **2000**, *16*, 5123−5129.
(2) Blodgett, K. B. *J. Am. Chem. Soc.* **1935**, *57*, 1007.
(3) Roberts, G. G. *Langmuir−Blodgett Films*; Plenum Press: New York, 1990.
(4) Ulman, A. *An Introduction to Ultrathin Organic Films: From Langmuir−Blodgett to Self-Assembly*; Academic Press: Boston, 1991.
(5) Byrd, H.; Pike, J. K.; Talham, D. R. *Chem. Mater.* **1993**, *5*, 709−715.
(6) Byrd, H.; Whipps, S.; Pike, J. K.; Ma, J.; Nagler, S. E.; Talham, D. R. *J. Am. Chem. Soc.* **1994**, *116*, 295−301.
(7) Byrd, H.; Pike, J. K.; Talham, D. R. *J. Am. Chem. Soc.* **1994**, *116*, 7903−7904.
(8) Seip, C. T.; Byrd, H.; Talham, D. R. *Inorg. Chem.* **1996**, *35*, 3479−3483.
(9) Seip, C. T.; Granroth, G. E.; Meisel, M. W.; Talham, D. R. *J. Am. Chem. Soc.* **1997**, *119*, 7084−7094.
(10) Fanucci, G. E.; Seip, C. T.; Petruska, M. A.; Nixon, C. M.; Ravaine, S.; Talham, D. R. *Thin Solid Films* **1998**, *327−329*, 331−335.
(11) Fanucci, G. E.; Talham, D. R. *Langmuir* **1999**, *15*, 3289−3295.
(12) Fanucci, G. E.; Petruska, M. A.; Meisel, M. W.; Talham, D. R. *J. Solid State Chem.* **1999**, *145*, 443−451.
(13) Petruska, M. A.; Fanucci, G. E.; Talham, D. R. *Chem. Mater.* **1998**, *10*, 177−189.
(14) Petruska, M. A.; Fanucci, G. E.; Talham, D. R. *Thin Solid Films* **1998**, *327−329*, 131−135.
(15) Petruska, M. A.; Talham, D. R. *Chem. Mater.* **1998**, *10*, 3673−3682.
(16) Petruska, M. A. Organic/Inorganic Langmuir−Blodgett Films Based on Metal Phosphonates. Ph.D. thesis, University of Florida, Gainesville, FL, 2000; p 258.
(17) Cunningham, D.; Hennelly, P. J. D. *Inorg. Chim. Acta* **1979**, *37*, 95−102.
(18) Cao, G.; Lee, H.; Lynch, V. M.; Mallouk, T. E. *Inorg. Chem.* **1988**, *27*, 2781−2785.
(19) Cao, G.; Lee, H.; Lynch, V. M.; Mallouk, T. E. *Solid State Ionics* **1988**, *26*, 63−69.

10.1021/cm0106623 CCC: $22.00
Published on Web 04/24/2002

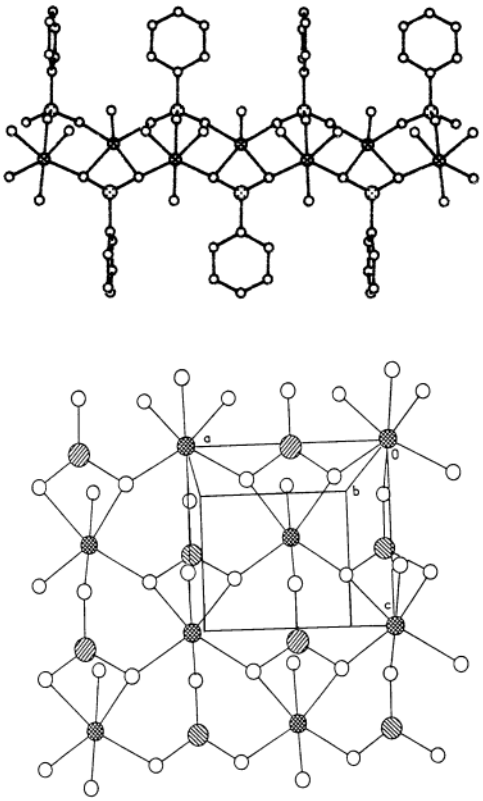

Figure 1. Two views of $Mn(O_3PC_6H_5)H_2O$: (top) in cross section showing the layered nature of the structure and (bottom) perpendicular to the Mn^{2+} ion plane showing the nearly square grid metal phosphonate network. Key: oxygen, small open circles; manganese, cross-hatched circles; phosphorus, diagonal-hatched circles. Phosphorus atoms above and below the plane are distinguished by hatch marks with different directions. Adapted from ref 18 and 61.

temperatures (12−18.5 K, depending on the phosphonate ligand), these manganese salts order as canted antiferromagnets, sometimes called weak ferromagnets, where antiferromagnetically coupled nearest-neighbor moments do not completely cancel as a result of spin canting that arises from the low site symmetry of the ions.[20,21] The characteristic magnetic behavior of the manganese phosphonate solids has been reproduced in LB films of octadecylphosphonic acid.[8,9] Similarly, manganese phosphonate LB films incorporating phenoxy and azobenzyloxy groups have also demonstrated the same long-range magnetic ordering as their alkylphosphonate solid-state counterparts.[12,16]

A significant step will be to demonstrate "dual-network" assemblies where the organic and inorganic networks both contribute properties to the LB film.[22,23] Working toward this goal, we have prepared manganese phosphonate LB films based on the tetrathiafulvalene (TTF) amphiphile **1**. TTF cation radicals and related ions form conducting and superconducting networks in the solid state[24−28] and, in some cases, have been shown to form conducting LB films.[29−38] Manganese phosphonate LB films of **1** could produce "dual-network" assemblies where the organic network is conducting and the inorganic network is magnetic. In this report, manganese phosphonate films of **1** are described along with structural and physical properties characterization that is aided by comparison of the LB films to analogous solid-state compounds, including salts of the "model" compound **2**. We show that the rational design of the bis(phosphonic acid) molecules **1** and **2** leads to the formation of manganese salts that have an inorganic lattice similar to the networks observed for the mono(phosphonate) parent compounds. While the inorganic lattice type based on mono(phosphonate) ligands has the formula $Mn(O_3PR)H_2O$, the same structure formed with a bis(phosphonate) has the formula $Mn_2(L)(H_2O)_2$, where L is the bis(phosphonate) ligand **1** or **2**. Like the simpler manganese phosphonates, the TTF analogues become magnetic at low temperatures.

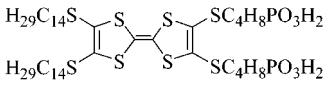

1

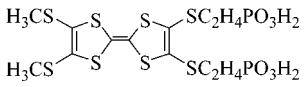

2

Experimental Section

Synthesis of Organic and Inorganic Compounds. Unless otherwise indicated, all reagents were purchased from either Aldrich (Milwaukee, WI) or Fisher Scientific (Pittsburgh, PA) and used as received. All reactions were performed under Ar or N_2 with glassware dried in an oven at 140 °C overnight unless otherwise specified. Dichloromethane was dried over P_2O_5 and freshly distilled prior to use. Tetrahydrofuran was dried over sodium benzophenone ketyl radical and freshly distilled prior to use. Triethyl phosphite was dried and distilled over Na. Triethylamine was dried and distilled over CaH_2. Methanol was dried and distilled over Mg. Compounds

(20) Carling, S. G.; Day, P.; Visser, D.; Kremer, R. K. *J. Solid State Chem.* **1993**, *106*, 111−119.
(21) Carling, S. G.; Day, P.; Visser, D. *J. Phys.: Condens. Matter* **1995**, *7*, L109−L113.
(22) Clemente-León, M.; Coronado, E.; Delhaes, P.; Gómez-Garcia, C. J.; Mingotaud, C. *Adv. Mater.* **2001**, *13*, 574−577.
(23) Talham, D. R.; Seip, C. T.; Whipps, S.; Fanucci, G. E.; Petruska, M. A.; Byrd, H. *Comments Inorg. Chem.* **1997**, *19*, 133−151.
(24) Ferraris, J.; Cowan, D. O.; Walatka, V., Jr.; Perlstein, J. H. *J. Am. Chem. Soc.* **1973**, *95*, 948.
(25) Bechgaard, K.; Jacobsen, C. S.; Mortensen, K.; Pedersen, M. J.; Thorup, N. *Solid State Commun.* **1980**, *33*, 1119−1125.
(26) Bechgaard, K.; Carneiro, K.; Rasmussen, F. G.; Olsen, K.; Rindorf, G.; Jacobsen, C. S.; Pederson, H. J.; Scott, J. E. *J. Am. Chem. Soc.* **1981**, *103*, 2440.
(27) Wudl, F.; Wobschall, D.; Hufnagel, E. J. *J. Am. Chem. Soc.* **1972**, *94*, 670−672.
(28) Williams, J. M.; Ferraro, J. R.; Thorn, R. J.; Carlson, K. D.; Geiser, U.; Wang, H. H.; Kini, A. M.; Whangbo, M.-H. *Organic Superconductors*; Simon & Schuster: Englewood Cliffs, NJ, 1992.
(29) Bryce, M. R.; Petty, M. C. *Nature* **1995**, *374*, 771−776.
(30) Nakamura, T. Electrically Conductive Langmuir−Blodgett Films. In *Handbook of Organic Conductive Molecules and Polymers*; Nalwa, H. S., Ed.; John Wiley and Sons Ltd.: Chichester, U.K., 1997; Vol. 1, pp 727−779.
(31) Vandevyver, M. *Thin Solid Films* **1992**, *210/211*, 240−245.
(32) Vandevyver, M.; Roulliay, M.; Bourgoin, J. P.; Barraud, A.; Gionis, V.; Kakoussis, V. C.; Mousdis, G. A.; Morand, J.-P.; Noel, O. *J. Phys. Chem.* **1991**, *95*, 246−251.
(33) Vandevyver, M.; Roulliay, M.; Bourgoin, J.-P.; Barraud, A.; Morand, J. P.; Noel, O. *J. Colloid Interface Sci.* **1991**, *141*, 459−466.
(34) Dourthe, C.; Izumi, M.; Garrigou-Lagrange, C.; Buffeteau, T.; Desbat, B.; Delhaes, P. *J. Phys. Chem.* **1992**, *96*, 2812−2820.
(35) Ohnuki, H.; Noda, T.; Izumi, M.; Imakubo, T.; Kato, R. *Supramol. Science* **1997**, *4*, 413−416.
(36) Ohnuki, H.; Noda, T.; Izumi, M.; Imakubo, T.; Kato, R. *Phys. Rev. B* **1997**, *55*, R10225−R10228.
(37) Ohnuki, H. Studies on Metallic Conducting Langmuir−Blodgett Films of Tetrathiafulvalene Derivatives. Ph.D. Thesis, Tokyo University of Mercantile Marine, Tokyo, 1998.
(38) Ohnuki, H.; Nagata, M.; Ishizaki, Y.; Imakubo, T.; Kobayashi, K.; Kato, R.; Izumi, M. *Synth. Met.* **1999**, *102*, 1699−1700.

bis(tetraethylammonium)bis(2-thioxo-1,3-dithiole-4,5-dithiolato)zincate (**4**),[39] 4,5-bis(tetradecylthio)-1,3-dithiole-2-thione (**5**),[40] 4,5-bis(methylthio)-1,3-dithiole-2-thione (**6**),[40] 4,5-bis[(2′-cyanoethyl)thio]-1,3-dithiole-2-thione (**8**),[40] 4,5-bis[(2′-cyanoethyl)thio]-1,3-dithiole-2-one (**9**),[41,42] and 2,3-bis[(2′-cyanoethyl)thio]-6,7-bis(methylthio)tetrathiafulvalene (**11**)[40] were prepared as previously described. Manganese chloride tetrahydrate, 99.6%, was purchased from Fisher. Manganese butylphosphonate was prepared as previously described.[18]

Diethyl (4-Bromobutyl)phosphonate (3). A mixture of dibromobutane (50 g, 0.23 mol) and triethyl phosphite (20 mL, 0.12 mol) was allowed to reflux overnight. The next morning low-boiling impurities and remaining triethyl phosphite were removed in vacuo. Column chromatography on silica in a pentane/diethyl ether mobile phase eluted the dibromobutane starting material. The product was eluted with 1:1 acetone/diethyl ether [R_f (2:1 acetone/diethyl ether) = 0.80], and concentration of this fraction afforded the product as a nearly pure, colorless liquid in 39% yield. ^{1}H NMR ($CDCl_3$) δ 4.08 (m, 4H), 3.39 (t, 2H), 1.94 (m, 2H), 1.74 (m, 4H), 1.30 (t, 6H); ^{13}C NMR ($CDCl_3$) δ 61.5, 61.4, 33.1, 32.9, 32.7, 25.6, 23.8, 21.1, 16.4, 16.3; HRMS (FAB) found *m*/*z* 273.0237, calcd for $C_8H_{19}O_3PBr$ *m*/*z* 273.0255 (M^+).

4,5-Bis[[4′-(diethoxyphosphinyl)butyl]thio]-1,3-dithiole-2-thione (7). To a solution of **4** (3.94 g, 5.5 mmol) in 150 mL of acetone was added dropwise from an addition funnel a solution of **3** (6 g, 0.022 mol) in 80 mL of acetone. The dark pink solution was allowed to stir for 3 days. At this time water was added, and the mixture was extracted three times with 100 mL of diethyl ether. The organic layers were collected and washed with 200 mL of water, dried over $MgSO_4$, and concentrated in vacuo. Column chromatography of the brown oil on silica in 100% diethyl ether eluted impurities. Increasing the polarity of the eluent to 1:1 acetone/diethyl ether eluted an orange band [R_f (1:1 acetone/diethyl ether) = 0.69]. Concentration of this fraction gave the product as a nearly pure, orange oil in 50% yield. ^{1}H NMR ($CDCl_3$) δ 4.09 (m, 8H), 2.87 (t, 4 H), 1.74 (m, 12H), 1.32 (t, 12H); ^{13}C NMR ($CDCl_3$) δ 210.2, 135.6, 61.0, 60.9, 35.4, 29.7, 29.5, 25.3, 23.5, 20.9, 20.8, 16.0, 15.9, 15.9, 15.8; HRMS (FAB) found *m*/*z* 583.0663, calcd for $C_{19}H_{37}O_6P_2S_8$ *m*/*z* 583.0669 (M^+).

2,3-Bis[[4′-(diethoxyphosphinyl)butyl]thio]-6,7-bis(tetradecylthio)tetrathiafulvalene (10). A round-bottomed flask was charged with **7** (0.61 g, 1.1 mmol), **5** (0.62 g, 1.1 mmol), excess triethyl phosphite (1.5 mL), and benzene (6 mL), and the resulting mixture was allowed to reflux for 3 days. Removal of the benzene in vacuo left a red residue, which was subjected to column chromatography on silica. The initial bands were eluted with 100% diethyl ether, and the polarity of the eluent was increased to 3:2 diethyl ether/acetone to remove a red band. Concentration of this fraction in vacuo gave a red oil determined to be the nearly pure product in 17% yield. ^{1}H NMR ($CDCl_3$) δ 3.92 (m, 8H), 2.67 (m, 8H), 1.56−1.74 (s, 12H), 1.46 (m, 4H), 1.22 (m, 4H), 1.16 (t, 12H), 1.04−1.1.18 (s, 40H), 0.71 (t, 6H); ^{13}C NMR ($CDCl_3$) δ 210.2, 135.6, 61.0, 60.9, 35.4, 29.7, 29.5, 25.3, 23.5, 20.9, 20.8, 16.0, 15.9, 15.9, 15.8; HRMS (FAB) found *m*/*z* 1108.4273, calcd for $C_{50}H_{94}O_6P_2S_8$ *m*/*z* 1108.4292 (M).

2,3-Bis[4′-phosphonobutyl)thio]-6,7-bis(tetradecylthio)tetrathiafulvalene (1). To a solution of **10** (0.2 g, 0.20 mmol) in 10 mL of dichloromethane was added triethylamine (0.23 mL, 8 equiv) and bromotrimethylsilane (0.22 mL, 7 equiv). After stirring for 6 h, the solution was concentrated in vacuo, and 10 mL of methanol was added to the residue. Stirring was continued for 15 h when the brownish-orange precipitate was collected and washed with water and diethyl ether. The yield was 78%. Mp (*s*95 °C) 193−194 °C; IR (KBr, cm^{-1}) 3406 (br), 2955, 2918, 2850, 2334 (br), 1683 (br), 1469, 1415, 1259, 1101, 1020, 987, 887, 802, 771, 717; UV−vis λ_{max} ($CHCl_3$/CH_3CH_2OH) 267 nm (ϵ = 15 800 M^{-1} cm^{-1}), 310 nm (ϵ = 13 400 M^{-1} cm^{-1}), 334 nm (ϵ = 13 600 M^{-1} cm^{-1}), 386 nm (sh) (ϵ = 3500 M^{-1} cm^{-1}), 472 nm (sh) (ϵ = 600 M^{-1} cm^{-1}); HRMS (FAB) found *m*/*z* 996.3001, calcd for $C_{42}H_{78}O_6P_2S_8$ *m*/*z* 996.3039 (M). Anal. Calcd for $C_{42}H_{78}O_6P_2S_8$: C, 50.60; H, 7.83. Found: C, 50.54; H, 8.23. Cyclic voltammetry (benzonitrile, 0.1 V/s, Bu_4NPF_6, vs Ag/$AgNO_3$) E_1 = 0.21 V (rev), E_2 = 0.49 V (rev).

2,3-Bis[[2′-(diethoxyphosphinyl)ethyl]thio]-6,7-bis(methylthio)tetrathiafulvalene (12). A solution of **11** (0.68 g, 1.4 mmol) in 50 mL of THF was degassed for 30 min. At this time a solution of cesium hydroxide monohydrate (0.53 g, 3.2 mmol) in 10 mL of methanol was added dropwise from an addition funnel over 30 min. During the course of this addition, a precipitate became evident in the flask. After the mixture was stirred for an additional 30 min, diethyl (2-bromoethyl)-phosphonate (0.58 mL, 3.2 mmol) was added. The resulting mixture was stirred for 1 h, after which time the solvent was removed in vacuo. Column chromatography of the residue in 3:2 acetone/diethyl ether eluted a red band [R_f (3:2 diethyl ether/acetone) = 0.6], which upon concentration was the product as a nearly pure, red oil in 65% yield. ^{1}H NMR ($CDCl_3$) δ 4.11 (m, 8H), 3.02 (m, 4H), 2.43 (s, 6H), 2.09 (m, 4H), 1.34 (t, 12H); ^{13}C ($CDCl_3$) δ 127.7, 127.4, 112.2, 109.6, 61.9, 61.8, 29.2, 29.2, 27.7, 25.9, 19.1, 16.4, 16.3; HRMS (FAB) found *m*/*z* 687.9585, calcd for $C_{20}H_{34}O_6P_2S_8$ *m*/*z* 687.9596 (M).

2,3-Bis[(2′-phosphonoethyl)thio]-6,7-bis(methylthio)-tetrathiafulvalene (2). To a solution of **12** (0.32 g, 0.47 mmol) in 10 mL of dichloromethane was added triethylamine (3.1 mL, 48 equiv) and bromotrimethylsilane (2.3 mL, 38 equiv). After stirring overnight, the solution was concentrated in vacuo, and 10 mL of methanol was added to the residue. Stirring was continued for 24 h, at which time the mustard-yellow solid was collected and washed with water and diethyl ether. The yield was 90%. Mp 179−181 °C; IR (KBr, cm^{-1}) 3447 (br), 2982, 2929, 2335 (br), 1662, 1473, 1421, 1296, 1201, 1151, 995, 950, 883, 769, 717, 684; HRMS (FAB) found *m*/*z* 575.8349, calcd for $C_{12}H_{18}O_6P_2S_8$ *m*/*z* 575.8344 (M). Anal. Calcd for $C_{12}H_{18}O_6P_2S_8 \cdot 0.6C_6H_{15}N$: C, 29.41; H, 4.24; N, 1.32. Found: C, 29.59; H, 4.45; N, 1.43.

Manganese 2,3-Bis[(2′-phosphonoethyl)thio]-6,7-bis(methylthio)tetrathiafulvalene [Mn_2(2)(H_2O)$_2$]. To a solution of **2** (0.024 g, 0.04 mmol) in 15 mL of water (in which the pH was adjusted to between 4 and 5 with 0.1 M KOH and 0.1 M HCl) was added manganese chloride tetrahydrate (0.018 g, 0.09 mmol) in 15 mL of water (in which the pH was adjusted to 5). A brown solid immediately precipitated from solution. The reaction mixture was stirred at 70 °C overnight. The next day 0.02 mg of brown solid was collected and washed with water and diethyl ether. IR (cm^{-1}) 3478, 1614, 1419, 1288, 1261, 1204, 1166, 1085, 993, 890, 801, 773, 727, 543. Anal. Calcd for $C_{12}H_{18}O_8P_2S_8Mn_2$: C, 20.03; H, 2.51. Found: C, 19.63; H, 2.16.

Methods and Instrumentation for characterizing molecules and LB films have all been detailed in prior publications.[1,13−15]

Results

TTF Phosphonic Acids and Salts. The synthesis of amphiphile **1** relies on the cross-coupling of two functionalized thiones.[40,43−47] In this case thiones **5**[40]

(39) Hansen, T. K.; Becher, J.; Jorgensen, T.; Varma, K. S.; Khedekar, R.; Cava, M. P. Bis-(Ethylenedithio)-Tetrathiafulvalene (BEDT-TTF). In *Organic Synthesis*; Boeckman, J. R. K., Ed.; John Wiley and Sons: New York, 1996; Vol. 73, p 270.

(40) Simonsen, K. B.; Svenstrup, N.; Lau, J.; Simonsen, O.; Mork, P.; Kristensen, G. J.; Becher, J. *Synthesis* **1996**, 407−418.

(41) Svenstrup, N.; Rasmussen, K. M.; Hansen, T. K.; Becher, J. *Synthesis* **1994**, 809−812.

(42) Kumasaki, M.; Tanaka, H.; Kobayashi, A. *J. Mater. Chem.* **1998**, *8*, 301−307.

(43) Krief, A. *Tetrahedron* **1986**, *42*, 1209−1252.

(44) Narita, M.; Pittman, J. C. U. *Synthesis* **1976**, 489−514.

(45) Papavassiliou, G. C.; Zambonis, J. S.; Mousdis, G. A.; Yiannopoulos, S. Y. *Mol. Cryst. Liq. Cryst.* **1988**, *156*, 269−276.

(46) Yoneda, S.; Kawase, T.; Inaba, M.; Yoshida, Z. *J. Org. Chem.* **1978**, *43*, 595−598.

(47) McCullough, R. D.; Petruska, M. A.; Belot, J. A. *Tetrahedron* **1999**, *55*, 9979−9998.

Scheme 1. Synthesis of Molecules 1 and 2[a]

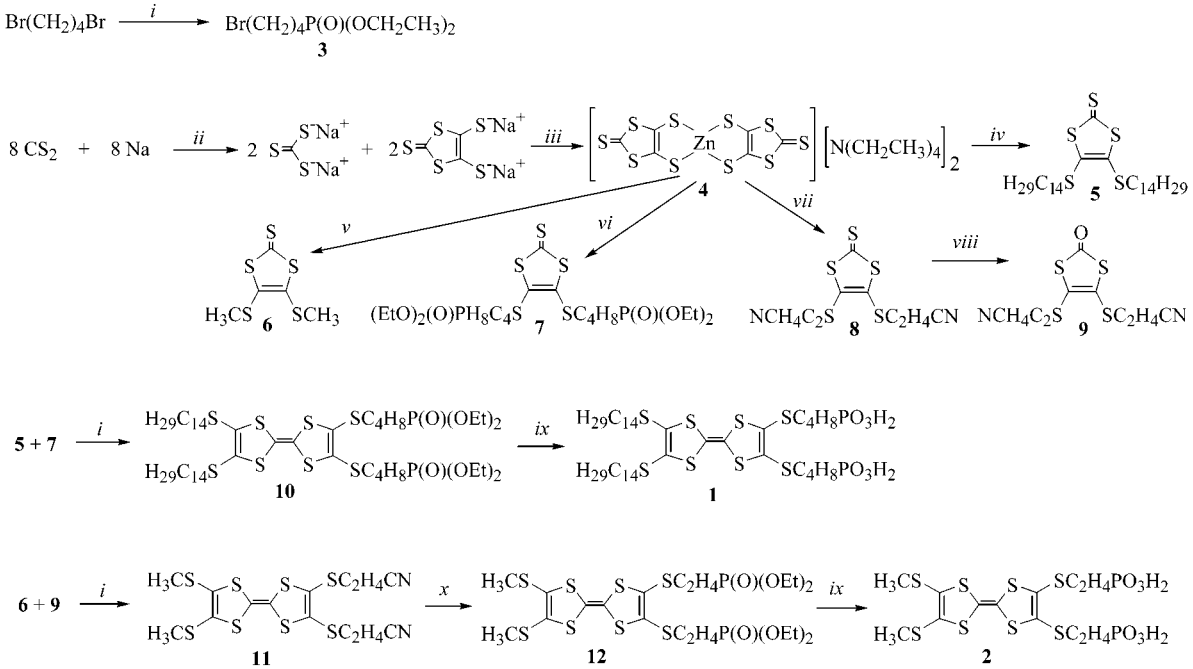

[a] (i) $P(OCH_2CH_3)_3$, Δ. (ii) DMF. (iii) $ZnCl_2$, $N(CH_2CH_3)_4Br$. (iv) $BrC_{14}H_{29}$, CH_3CN. (v) ICH_3, CH_3CN. (vi) **3**, $CH_3C(O)CH_3$. (vii) $Br(CH_2)_2CN$, CH_3CN. (viii) $Hg(OAc)_2$, $CHCl_3/CH_3COOH$. (ix) (1) $BrSi(CH_3)_3$, $N(CH_2CH_3)_3$; (2) CH_3OH. (x) (1) $CsOH(H_2O)$; (2) $BrC_2H_4P(O)(OEt)_2$.

and **7** were first prepared from the $Zn(dmit)_2$ precursor,[39] as shown in Scheme 1. Coupling of the thiones gives the unsymmetrical product in modest yield, and hydrolysis of the phosphonate esters with bromotrimethylsilane and methanol conveniently affords the bis(phosphonic acid) derivative of TTF.[48−50] Compound **1** and its solid-state model **2** have also been prepared from cyanoethyl-protected TTF dithiolates following procedures described by Becher and co-workers.[40,41,51] The cyanoethyl groups are easily removed with cesium hydroxide, and the resulting dithiolate anions can be quenched with the alkyl bromide reagent. Precipitation of the manganese phosphonate salts of **2** followed procedures described by Cao et al.[18] for the syntheses of metal phosphonate salts of phenylphosphonic acid with various divalent metal ions.

Langmuir Monolayers of 1. The behavior of amphiphile **1** at the air/water interface, which is characterized by its pressure vs mean molecular area isotherm, is in agreement with the substitution pattern of the molecule. The isotherm (Figure 2) shows an apparent liquid-condensed phase that collapses at a mean molecular area near 44 Å^2. This area reflects the presence of the two hydrocarbon chains on each molecule and is consistent with a nearly upright positioning of the TTF moiety on the water surface, with very little tilt from the surface normal. Amphiphile **1** has two phosphonic acid substituents, and it is likely that both of these groups are at the water surface, forcing the TTF moiety to stand nearly upright. Heating the subphase induces

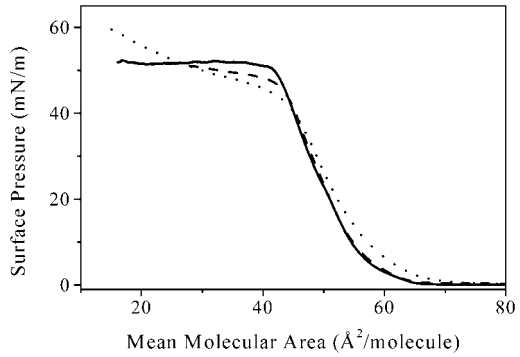

Figure 2. Pressure vs mean molecular area isotherms for **1** on a pure water subphase at room temperature (solid line), on a water subphase heated to 40 °C (dashed line), and on a water subphase containing 0.5 mM Mn^{2+}, heated to 35 °C (dotted line). The spreading solutions had concentrations of 0.4−0.6 mg/mL in 10% ethanol/chloroform. The isotherms were recorded with a linear compression rate of 8 mN/(mm/min) and with maximum barrier speeds of 20 mm/min.

only minor changes in the shape of the isotherm, as observed in Figure 2. Upon addition of Mn^{2+} to the subphase, the monolayer behavior depends significantly on pH, consistent with observations on other organophosphonate Langmuir monolayers.[10−12]

LB Films of 1 with Manganese(2+). *Film Deposition.* Langmuir monolayers of organophosphonate amphiphiles quickly become rigid when acidic metal ions are added to the subphase.[9−11] However, under appropriate conditions, the monolayers can be maintained with sufficient fluidity to allow conventional vertical deposition, with crystallization of the metal phosphonate continuous lattice within the transferred bilayers. For the transfer of **1** with Mn^{2+} ions, we find that transfer is optimized within a pH range of 5.7−5.8 at 35 °C. The higher temperature decreases the rigidity of the monolayer at the air/water interface and may help

(48) McKenna, C. E.; Higa, M. T.; Cheung, N. H.; McKenna, M.-C. *Tetrahedron Lett.* **1977**, 155−158.
(49) Katz, H. E.; Bent, S. F.; Wilson, W. L.; Schilling, M. L.; Ungashe, S. B. *J. Am. Chem. Soc.* **1994**, *116*, 6631−6635.
(50) Katz, H. E.; Wilson, W. L.; Scheller, G. *J. Am. Chem. Soc.* **1994**, *116*, 6636−6640.
(51) Lau, J.; Simonsen, O.; Becher, J. *Synthesis* **1995**, 521−526.

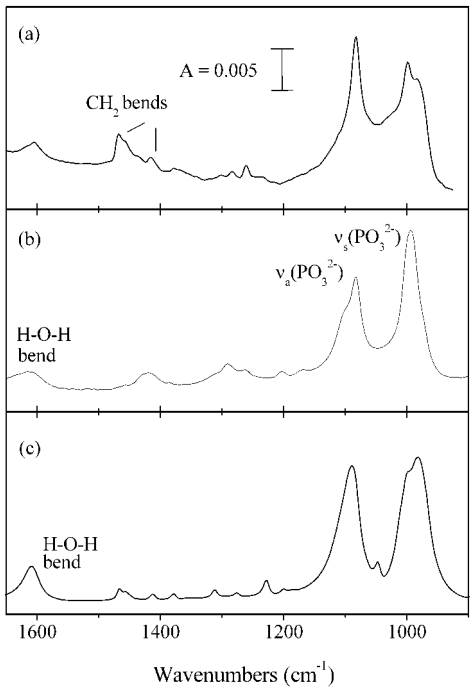

Figure 3. (a) ATR-FTIR spectrum of a three-bilayer LB film sample of **1** with manganese (2+), (b) FTIR spectrum of a KBr pellet of the manganese(2+) salt of **2**, and (c) FTIR spectrum of manganese butylphosphonate. Band assignments are discussed in the text. The similarities in the shape and energies of the phosphonate stretches suggest similar metal phosphonate lattices in the solid and film samples.

anneal the manganese phosphonate lattice upon transfer. The film is deposited with dipping speeds of 5 and 3 mm/min on the down- and upstrokes, respectively.

Infrared and Optical Spectroscopy. An attenuated total reflectance Fourier transform infrared (ATR−FTIR) spectrum of a three-bilayer LB film sample of the manganese phosphonate LB film of **1** is shown in Figure 3. For comparison, the IR spectrum of the solid-state manganese butylphosphonate ($Mn(O_3PC_4H_9)H_2O$) is added. The phosphonate stretches, which appear between 900 and 1200 cm^{-1} in the layered metal phosphonates, are similar in the film and butylphosphonate powder. We have previously used these modes to fingerprint the metal phosphonate structure type, as these stretches are sensitive to the metal phosphonate binding geometry.[9−12,15] In manganese butylphosphonate, the asymmetric and symmetric phosphonate stretches are found near 1087 and 984 cm^{-1}, respectively. There is a shoulder on the high-energy side of the 984 cm^{-1} band that is attributed to the low site symmetry of the phosphonate. In the manganese LB film of **1**, these bands appear at 1084 cm^{-1} for the asymmetric and 997 and 986 cm^{-1} for the symmetric modes, suggesting similar metal phosphonate binding geometries in the two materials.

In addition to the phosphonate stretches, other modes are present in the IR spectrum of the TTF molecule. Bands at 1467 and 1413 cm^{-1} are assigned as C−H bending modes for the alkyl chains, and the latter mode corresponds to those methylene groups with neighboring sulfur atoms on the TTF core. Although not shown, the asymmetric and symmetric methylene stretches are observed at 2920 and 2851 cm^{-1}, respectively. These peak positions and the full width at half-maximum

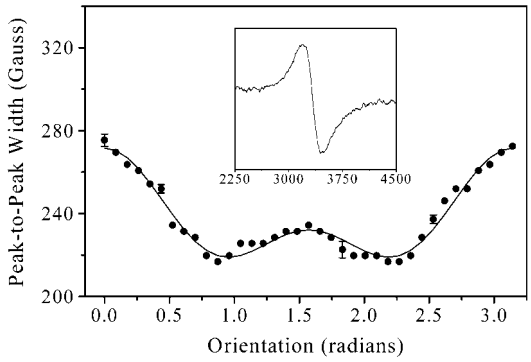

Figure 4. Room-temperature ESR line width as a function of sample orientation for a 100-bilayer LB film sample of **1** transferred with Mn^{2+}. The solid line is a fit to the data with $\Delta H_{P-P} = A + B(3\cos^2\phi - 1)^2$ with $A = 219$ G and $B = 13$ G, where ϕ is the angle between the applied magnetic field and the normal to the film surface. The fit shows antiferromagnetic exchange in a two-dimensional lattice. The room-temperature ESR signal is seen in the inset, taken with the applied field (gauss) parallel to the surface normal.

(fwhm) of the asymmetric methylene stretch, 20 cm^{-1}, indicate that the 14-carbon alkyl chains are ordered and close-packed in this film.[52,53] It is likely that there is disorder among the four-carbon tethers linking the phosphonic acid headgroups to the TTF core, similar to observations on related systems described previously.[13,15] The H−O−H stretch observed near 3500 cm^{-1} and the water bend at 1608 cm^{-1} confirm the presence of the coordinated water molecule expected with the $Mn(O_3PR)H_2O$ lattice type.

The TTF moiety gives rise to UV−vis absorbance bands located near 275, 315, 405, and 522 nm, and the intensity of these bands increases linearly with the number of layers deposited. In general the bands broaden and shift red a few nanometers relative to the solution spectra. The absorbances correspond to intramolecular electronic transitions within the neutral TTF unit, and the higher energy bands (275 and 315 nm) are assigned to $\pi-\pi^*$ transitions.[54,55]

Magnetic Properties of the Mn^{2+} LB Film of 1. Electron spin resonance (ESR) measurements were made on a 100-bilayer LB film sample on Mylar. The Mn^{2+} ESR signal is dipolar-broadened, as expected for an exchange-coupled lattice of manganese ions. An example of this signal is shown in the inset in Figure 4. The substrate was cut into strips that were then stacked and arranged vertically in an ESR tube so that the sample could be rotated with respect to the magnetic field. During this experiment, the *g*-values change only slightly within the range 1.99−2.00. In contrast to the solid-state powders, LB film samples can be aligned in the ESR experiment. As the sample is rotated in the magnetic field, the room-temperature peak-to-peak width (ΔH_{P-P}) changes, and the response can be fit with an expression for the angular dependence of the line width in a two-dimensional, exchange-coupled antifer-

(52) Maoz, R.; Sagiv, J. *J. Colloid Interface Sci.* **1984**, *100*, 465−496.
(53) Tillman, N.; Ulman, A.; Schildkraut, J. S.; Penner, T. L. *J. Am. Chem. Soc.* **1988**, *110*, 6136−6144.
(54) Richard, J.; Vandevyver, M.; Barraud, A.; Morand, J. P.; Delhaes, P. *J. Colloid Interface Sci.* **1989**, *129*, 254−257.
(55) Cea, P.; Lafuente, C.; Urieta, J. S.; Lopez, M. C.; Royo, F. M. *Langmuir* **1997**, *13*, 4892−4897.

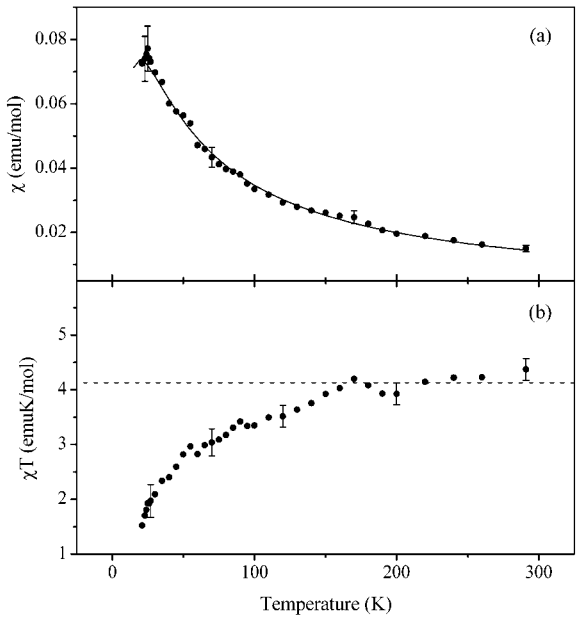

Figure 5. (a) Temperature dependence of the integrated area of the ESR signal for a 100-bilayer LB film sample of **1** transferred with Mn^{2+}. The room temperature point has been set to the expected spin-only value of the susceptibility for Mn^{2+}. The solid line is a fit to the data with the numerical expression for Heisenberg antiferromagnetic exchange in a two-dimensional lattice. The fit yields a nearest-neighbor exchange constant $J/k_B = -2.3$ K, which is similar to exchange constants determined for other manganese phosphonate solid-state materials and LB films. (b) Temperature dependence of the product χT for the same sample. The decrease at lower temperatures indicates antiferromagnetic exchange.

romagnet, $\Delta H_{P-P} = A + B(3\cos^2\phi - 1)^2$ (Figure 4),[56−58] with A and B equal to 219 and 13 G, respectively. In this equation, A and B include exchange and dipolar contributions to the line width, and ϕ is defined as the angle the applied magnetic field makes with the normal to the film surface. The angular dependence is characteristic of antiferromagnetic exchange in a two-dimensional lattice that is oriented parallel to the plane of the film and is consistent with observations on previous manganese organophosphonate LB films.[8,12,16]

Below 17 K, the signal becomes too broad for detection with X-band ESR spectroscopy. The integrated area of the ESR signal is proportional to its spin susceptibility,[59] and in Figure 5a, the ESR signal area is plotted as a function of temperature, with the room temperature point set equal to the expected spin-only value for Mn^{2+}. The data are fit to a series expansion for Heisenberg antiferromagnetic exchange in a two-dimensional lattice,[60] and an exchange constant $J/k_B = -2.3 \pm 0.1$ K is determined on the basis of the fit. This negative value for exchange suggests antiferromagnetic interactions as defined by the exchange Hamiltonian $H = -J\Sigma S_i S_j$, where the exchange is between nearest-neighbor spins i and j. This value is consistent with exchange constants determined for previously studied layered manganese

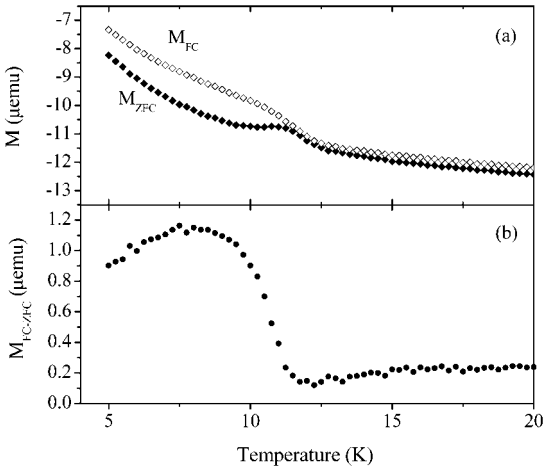

Figure 6. Magnetization vs temperature for a 100-bilayer LB film **1** transferred with Mn^{2+} with the measuring field applied parallel to the film plane. (a) Comparison of the data taken upon warming the film after cooling in zero applied field (ZFC) and cooling in a field of 1000 G (FC). For both cases, the measuring field is 100 G. (b) Difference in the FC and ZFC data, showing a net magnetization below 11.5 ± 0.5 K.

phosphonates that form with the structure $M(O_3PR)\cdot H_2O$,[9,12,16,20,61] adding further evidence for this network in the bis(phosphonate) LB film as well. Antiferromagnetic exchange is also evident in Figure 5b where the χT product is shown to decrease as the temperature is lowered.

Static susceptibility measurements obtained with superconducting quantum interference device (SQUID) magnetometry were used to probe magnetic ordering in the film. The 100-bilayer manganese phosphonate LB film sample of **1** was cut and oriented in a polyethylene vial with the applied magnetic field parallel to the film plane, and plots of the zero-field-cooled (ZFC) and field-cooled (FC) magnetization were obtained. Like related solid-state materials,[20,21] the magnetometry data indicate that there is a transition to canted antiferromagnetism in the manganese LB film of **1** that onsets at a Néel temperature (T_N) of 11.5 ± 0.2 K (here T_N is recorded at the discontinuity in the ZFC plot). In the FC−ZFC plot (Figure 6), a net magnetization is present below ordering, consistent with a canted antiferromagnetic state.[62] The sample was reoriented so that the applied field was perpendicular to the film plane, but the net magnetization is weaker in this orientation, indicating the canting moment lies within the planes. This result supports a spin orientation in the metal network of this LB sample that is the same as that observed in other materials forming the parent $M(O_3PR)H_2O$ lattice.

A spin-flop transition is observed in a plot of magnetization vs field when the film planes are arranged perpendicular to the applied field of the LB film sample. In this orientation, the applied field is parallel to the magnetic easy axis. The spin-flop transition is viewed as a discontinuity at 25 kG in the magnetization vs field plot ($T = 2$ K).[16] We have observed this transition at

(56) Gatteschi, D.; Sessoli, R. *Magn. Reson. Rev.* **1990**, *15*, 1−45.
(57) Patyal, B. R.; Willett, R. D. *Magn. Reson. Rev.* **1990**, *15*, 47−82.
(58) Richards, P. M.; Salamon, M. B. *Phys. Rev. B* **1974**, *9*, 32−45.
(59) de Jongh, L. J. *Introduction to Low-Dimensional Magnetic Systems*; de Jongh, L. J., Ed.; Kluwer Academic Publishers: Dordrecht, The Netherlands, 1990; pp 1−51.
(60) Lines, M. E. *J. Phys. Chem. Solids* **1970**, *31*, 101−116.
(61) Fanucci, G. E.; Krzystek, J.; Meisel, M. W.; Brunel, L.-C.; Talham, D. R. *J. Am. Chem. Soc.* **1998**, *120*, 5469−5479.
(62) In Figures 6 and 8, the slight increase in M_{FC-ZFC} as the temperature is raised from 4.5 K can be attributed to a combination of effects, including a distribution of T_N values due to the variance in domain sizes.

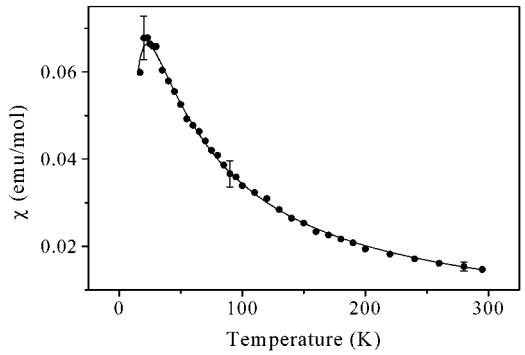

Figure 7. Temperature dependence of the integrated area of the ESR signal for Mn_2(**2**)$(H_2O)_2$. The room temperature point has been set to the expected spin-only value of the susceptibility for Mn^{2+}. The solid line is a fit to the data with the numerical expression for Heisenberg antiferromagnetic exchange in a two-dimensional lattice. The fit yields a nearest-neighbor exchange constant $J/k_B = -2.5$ K, a value similar to the exchange constant determined for the analogous LB film sample of **1**.

similar fields for other manganese phosphonate thin films that form the $Mn(O_3PR)H_2O$ lattice.[9,12,16]

Structural and Magnetic Characterization of the Manganese Salt of 2. The IR spectrum of a powdered sample of the Mn^{2+} salt of **2** is seen in Figure 3. The frequencies of the asymmetric and symmetric phosphonate stretches, 1085 and 993 cm^{-1}, respectively, suggest that the $M(O_3PR)H_2O$ network forms in the bis(phosphonate) solid-state compound as well as in the LB film sample. The H−O−H bending mode is observed near 1610 cm^{-1}, confirming water coordination, and peaks corresponding to C−H twisting, wagging, and bending modes are consistent with the presence of the TTF moiety. Combustion analysis and thermogravimetric analysis (TGA) results confirm the Mn_2(**2**)$(H_2O)_2$ stoichiometry, consistent with the $M(O_3PR)H_2O$ structure type, remembering that **2** is a bis(phosphonate) ligand.

The Mn^{2+} ESR signal is also dipolar-broadened for the Mn_2(**2**)$(H_2O)_2$ powder, and it appears similar to the signal obtained for the analogous LB film sample of **1**. Below 17 K the signal becomes too broad to detect, and this behavior is again characteristic of an approaching ordering transition. A plot of the temperature-dependent integrated area of the ESR signal, normalized to the spin-only value of the susceptibility at room temperature, for Mn_2(**2**)$(H_2O)_2$ is shown in Figure 7. By use of the same series expansion applied to the LB film data, a value for J/k_B of -2.5 ± 0.1 K is determined. Again the negative exchange constant indicates antiferromagnetic interactions, and the value is similar to what is seen for the manganese LB film of **1**, as well as for other manganese phosphonate solid-state materials and LB films that form with the structure $M(O_3PR)H_2O$. Evidence for magnetic ordering is also observed with SQUID magnetometry (Figure 8). A net magnetization is present in the FC−ZFC plot below the T_N of 11.2 ± 0.5 K, as seen in Figure 8b, again consistent with canted antiferromagnetism.

Discussion

LB Film Structure. Inorganic continuous solids are not very compressible, so in order to achieve such a

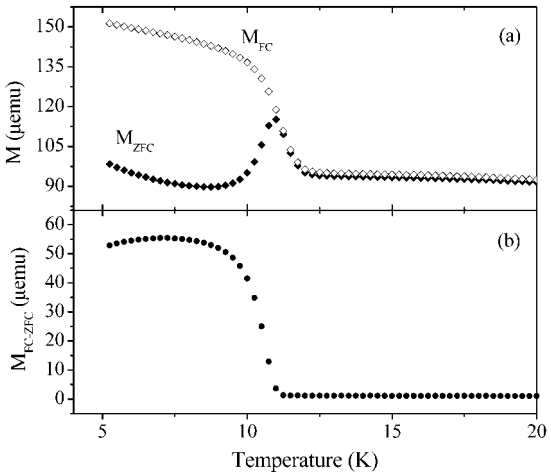

Figure 8. Magnetization vs temperature for 7.2 mg of a Mn_2(**2**)$(H_2O)_2$ powder. (a) Comparison of the data taken upon warming after cooling in zero applied field (ZFC) and cooling in a field of 1000 G (FC). For both cases, the measuring field is 100 G. (b) Difference in the FC and ZFC data, showing a net magnetization below 11.2 ± 0.5 K.

structure as part of an LB film, the amphiphilic ligands must be able to conform to the structural requirements of the inorganic lattice. In solid-state layered manganese phosphonates, such as the phenylphosphonate $Mn(O_3PC_6H_5)H_2O$, the "cross-sectional area" of a phosphonate group, with respect to the plane defined by the manganese ions, is approximately 28 $Å^2$ (Figure 1).[18] Normally, alkyl- and arylphosphonates have cross-sectional areas that are less than this, and when these groups are used as amphiphiles in LB films, the layers can expand to generate the $M(O_3PR)H_2O$ lattice in the transferred film.[9,12] Problems arise when the phosphonate groups cannot adopt the required spacing. If the phosphonates are packed too tightly, the $M(O_3PR)H_2O$ lattice will not form, and this can occur in LB films if the amphiphiles aggregate and restrict the phosphonate headgroups from achieving the required spacing.[15] At the same time, if the organic group is too bulky, then a different inorganic lattice is often adopted, and we have seen evidence for this with TTF derivatives substituted with a single phosphonate group that cannot be packed into the required space.[16] However, by including two phosphonic acid groups on the TTF core, the $M(O_3PR)H_2O$ structure forms in both LB films based on **1** and powdered solids based on **2**.

Bis(phosphonic acids) have been previously used to form a number of metal phosphonate salts. For example, 1,4-bis(phosphono)arylene ligands have been used to pillar layered zirconium and zinc phosphonates.[63−70]

(63) Clearfield, A. Metal Phosphonate Chemistry. In *Progress in Inorganic Chemistry*; John Wiley & Sons: New York, 1998; Vol. 47, pp 371−510.
(64) Clearfield, A. *Chem. Mater.* **1998**, *10*, 2801−2810.
(65) Alberti, G.; Casciola, M.; Costantino, U.; Vivani, R. *Adv. Mater.* **1996**, *8*, 291−303.
(66) Poojary, D. M.; Vermeulen, L. A.; Vicenzi, E.; Clearfield, A.; Thompson, M. E. *Chem. Mater.* **1994**, *6*, 1845−1849.
(67) Reis, K. P.; Joshi, V. K.; Thompson, M. E. *J. Catal.* **1996**, *161*, 62−67.
(68) Byrd, H.; Clearfield, A.; Poojary, D.; Reis, K. P.; Thompson, M. E. *Chem. Mater.* **1996**, *8*, 2239−2246.
(69) Zhang, B.; Poojary, D., M.; Clearfield, A. *Inorg. Chem.* **1998**, *37*, 1844−1852.
(70) Poojary, D. M.; Zhang, B.; Bellinghausen, P.; Clearfield, A. *Inorg. Chem.* **1996**, *35*, 5254−5263.

Metal phosphonates in which a bis(phosphonic acid) binds within the same layer are also known. Recently, Bujoli and co-workers[71] prepared a cadmium phosphonate salt of α,α′-*m*-xylenebis(phosphonic acid) in which the in-plane structure was reported to be similar to that of its cadmium mono(phosphonate) solid-state analogue. This result suggests that the spacings of the phosphonic acids in the α,α′-*m*-xylenebis(phosphonic acid) precursor are sufficient to allow for the $Cd(O_3PR)H_2O$ lattice to form. In contrast, we have observed that when the methylene phosphonic acid substituents are on aryl carbons neighboring each other, as in α,α′-*o*-xylenebis(phosphonic acid) (**13**), the phosphonic acids are not appropriately oriented to allow for the $Mn(O_3PR)H_2O$ structure to form.[16] However, if the length of the tether separating the aryl group from the phosphonic acid is increased, for example to the ethylthio spacer in the diacid **14**, the $M(O_3PR)H_2O$ lattice forms, now with stoichiometry $M_2L(H_2O)_2$, where L is the bis(phosphonate).[16] The thioethyl units impart sufficient flexibility to allow the phosphonate headgroups to adapt to the spacing required by the inorganic lattice. The geometry and dimensions of **14** make it a good model for the TTF-functionalized phosphonic acid **2**.

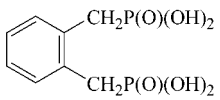

13

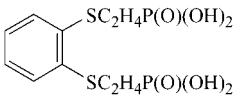

14

Manganese LB films of **1** have been deposited where the inorganic lattice is consistent with the $Mn(O_3PR)H_2O$ structure. This observation suggests that even on the water surface, where the appropriate orientation of the organic amphiphiles is required for crystallization of the metal phosphonate lattice, the spacing of the phosphonic acids is sufficient for inorganic lattice formation.

In the amphiphile, **1**, the spacer linking the TTF moiety and the phosphonic acid unit is a butylthio group rather than an ethylthio unit. The longer tether affords even more flexibility to the phosphonate groups, and the manganese phosphonate extended structure easily forms. The film contains both an inorganic continuous lattice and an organic molecular solid network, and in such films the optimum spacing in the two networks may differ. We have previously seen evidence for incommensurate organic and inorganic networks within metal phosphonate LB films containing azobenzene chromophores, in which the organic groups have a tendency to aggregate.[15] The flexible linker between the TTF core and the inorganic network accommodates any strain that may result if the two networks assume different packing geometries.

Magnetic Properties. The manganese phosphonate LB film based on **1** and the powdered solid based on **2** each order antiferromagnetically and the magnetic moments in the ordered state are due to spin canting, resulting in weak ferromagnetism. The magnetic properties provide support for formation of the two-dimensional $Mn(O_3PR)H_2O$ structure. This structure has been seen in several manganese organophosphonate solids[20,21] and LB films,[9,12,16] as well as in the purely inorganic $KMnPO_4$.[72,73] Each example orders as a canted antiferromagnet in the range $12\ K < T_N < 18.5\ K$. The ordering temperature is largely affected by electronic influences of the phosphonate or phosphate ligand,[61] but difficult-to-quantify structural differences may also play a role. The TTF phosphonate derivatives order just below this range, although the ordering temperature is close to that of manganese phenylphosphonate, which orders at 12 K.[61]

A possible explanation for the lower ordering temperature concerns the distance between layers, although previous studies have shown interlayer interactions do not significantly influence ordering in the manganese phosphonate series.[9] Furthermore, the salt of **2** and the LB film of **1** order at the same temperature yet have a different interlayer spacing. Another possibility is that the bis(phosphonates) cause a slight structural change in the manganese phosphonate layer. Small changes in bond angles and distances can influence the strength of superexchange interactions, such as those present in the manganese phosphonates. If adjacent phosphonate groups originate from the same molecule, there may be strain causing slight changes in bond angles and bond distances relative to the parent mono(phosphonate) analogues. However, the manganese(2+) salt of the bis(phosphonate) ligand **14** orders at 13.8 K,[16] similar to other manganese alkylphosphonates, and strain in this compound should be greater than in **1**, where the phosphonates are tethered with a butylthio group. The most likely explanation for the reduced ordering temperature is decreased structural and magnetic coherence length. It is possible that the incommensurate packing of the organic and inorganic networks, discussed above, limits domain size, thereby restricting the magnetic coherence length and suppressing the ordering temperature.

Oxidation of the Organic Network. While the inorganic lattice in these TTF-based organic/inorganic LB films provides magnetism, the possibility of introducing conductivity through the organic network now exists. However, our initial attempts to oxidize the TTF network have not resulted in a conducting film. The film is oxidized by I_2, and evidence for TTF^+ is seen in the visible spectrum. Unfortunately, this phase is not stable, and it quickly reverts to the neutral film by outgassing I_2. Postdeposition doping has been successful with some TTF-based LB films, but it does not always work.[29−38] If the structure is not optimized to accommodate a counterion, then it must reorganize. The presence of the inorganic lattice in the manganese phosphonate salts makes this reorganization difficult.

Conclusions

A mixed organic/inorganic Langmuir−Blodgett film has been developed containing an inorganic extended solid-state network and a functionalized organic molec-

(71) Penicaud, V.; Massiot, D.; Gelbard, G.; Odobel, F.; Bujoli, B. *J. Mol. Struct.* **1998**, *470*, 31−38.

(72) Visser, D.; Carling, S. G.; Day, P.; Deportes, J. *J. Appl. Phys.* **1991**, *69*, 6016−6018.

(73) Carling, S. G.; Day, P.; Visser, D. *Inorg. Chem.* **1995**, *34*, 3917−3927.

ular solid network. The film becomes magnetic at low temperature, due to ordering in the inorganic network, and the organic component has potential to become a conducting or semiconducting network. Additional work is required to develop stable films with partial oxidation of the organic network. Such "dual-network" assemblies will provide the chance to explore interactions between adjacent conducting and magnetic layers in "soft" thin film materials.

Acknowledgment. This work was supported by the National Science Foundation (NSF). M.A.P. acknowledges the NSF for a predoctoral fellowship.

CM0106623